Oxygen-Tolerant Alternating Copolymerization of Fluorinated Monomers and Vinyl Ethers at Mild Temperature

Minh-Loan Tran-Do, Jean-Pierre Habas, Bruno Ameduri

Oxygen-Tolerant Alternating Copolymerization of Fluorinated Monomers and Vinyl Ethers at Mild Temperature

Minh-Loan Tran-Do, Jean-Pierre Habas, Bruno Ameduri*

Institut Charles Gerhardt, Univ. Montpellier, CNRS, ENSCM, 34095 Montpellier, France.

E-mail: bruno.ameduri@enscm.fr

Abstract

The oxygen tolerant radical copolymerization of fluorinated monomers with vinyl ethers at room temperature in the presence of tri-*n*butylborane methoxypropylamine (TBBMOPA)/CH_3COOH system is presented. The combination of commercially available fluoroolefins (FO) [perfluoromethyl vinyl ether (PMVE) and hexafluoropropylene (HFP)] and vinyl ethers (VE) [ethyl vinyl ether (EVE) and 2-(perfluorohexyl)ethyl vinyl ether (FAVE6)] was used for the synthesis of different alternating poly(FO-*alt*-VE) copolymers (up to 43 % yield). The resulting copolymers were characterized by FT-IR, ^{19}F NMR and ^{1}H NMR spectroscopy techniques. Thermomechanical properties (T_g = -16 to 18 °C) of these polymers were also studied and justified in terms of structure-properties relationships. Their stabilities were investigated as a function of temperature by thermogravimetric analyses. Then, their degradation temperatures related to a weight loss of 5%, ($T_{d5\%}$) were evaluated as being comprised between 262 and 316 °C while poly(PMVE-*alt*-EVE) copolymer was characterized by a higher thermostability ($T_{d5\%}$ = 382 °C). Their surfaces were found to be hydrophobic, evidenced by water contact angle measured from 95 to 110 °. When soluble in SEC solvent, these fluorinated copolymers reached M_n up to 169,200 g mol^{-1}. Because of these features, such fluorinated copolymers may find applications in paints and coatings or as elastomers.

Keywords: fluorinated copolymers; radical polymerization; rheology; spectroscopic analyses; thermal properties; water angle angles.

1. Introduction

Fluoropolymers are specialty polymers endowed with exceptional properties which enable them to be involved in many high tech applications.[1–6] They are usually produced by radical copolymerization of fluorinated alkenes initiated by persulfate or peroxide at temperature higher than 50 °C. This polymerization requires the absence of oxygen that is regarded as a radical scavenger that inhibits this reaction. Thus, it was of interest to find out conditions at room temperature and in presence of oxygen to possibly enable the success of such a reaction. As a matter of fact, boranes have been found as being appropriate to initiate polymerization of fluoromonomers.[2,7–11] However, the experimental conditions may be hazardous, because of their pyrophoricity due to electro-deficient character. Nevertheless, borane BH_3 exhibits a high bond dissociation energy (BDE = 106.6 kcal mol^{-1}) to be used in organic reactions. As borane is a Lewis acid, complexing it with a Lewis base such as amine, phosphine[12] or carbene-based[13], efficiently reduces the B-H dissociation energy. In 1966, the first organoborane-amine complexes were reported as being air-tolerant.[14] Recently, Magenau and Wilson described an O_2-tolerant RAFT polymerization of alkyl methacrylates[15,16] and thiol-ene networks nanocomposites[17] at room temperature in the presence of tri-*n*butylborane methoxypropylamine (TBB-MOPA) (**Erreur ! Source du renvoi introuvable.**). This complex could release efficient TBB-MOPA which, successfully initiate a polymerization in presence of oxygen. TBB-MOPA bears an ether moiety, as hydrogen bond accepting group of amine, enhancing then the electron density of the latter complexing with the borane. Its decomplexation requires i) a reasonable heating energy (dissociation temperature at 63 °C) in the absence of a deblocking agent, also called “deblocker”,[18] or ii) in the presence of the deblocker (e.g. carboxylic acid or isocyanate), at room temperature, as reported by Magenau’s group.[15–17]

Actually, boranes play specific role in polymerization. They can be side groups of monomers promoting living radical polymerization.[19] As a matter of fact, the reactivity of electro-deficient boranes is blocked by the donating amine ligand.[18] The complex dissociation can occur under irradiation,[20] heating or in the presence of a deblocker, in order to generate in situ the reactive borane.[18]

On the other hand, the acceptor-donor copolymerization of electron withdrawing highly fluorinated olefins (FO), such as chlorotrifluoroethylene, hexafluoropropylene, tetrafluoroethylene and perfluoromethyl vinylether with electron donating vinyl ethers (VE), are known to lead to alternating poly(FO-*alt*-VE) copolymers.[21–30] As a matter of fact, fluoroolefins, such as perfluoromethyl vinyl ether (PMVE) and hexafluoropropylene (HFP), have an electron-acceptor character (e values for PMVE and HFP are 3.01 and 1.50,[31,32] respectively). Meanwhile, vinyl ethers are electron-donating ($-2.0 < e < -1.5$).[21,22,24]. Furthermore, both these families of monomers cannot be homopolymerized.

A higher yield is observed for the poly(PMVE-*alt*-EVE) copolymer when the feed molar ratio of comonomers is 1 : 1. This confirms previous studies on the alternating copolymer of CTFE with vinyl ether [34] or propylene[23,31] for which the rate of copolymerization is the highest.[31,34]

In that context, industrial productions of Lumiflon®[23] and Zeffle®,[33] used in resin coating with excellent chemical resistance have been achieved from radical copolymerization of vinyl ethers with chlorotrifluoroethylene or tetrafluoroethylene, respectively. Inspired from such above commercially available alternating copolymers,[23] our group has studied, since 2009, the copolymerization procedures of fluoroolefins with vinyl ethers using *tert*-butylperoxypivalate[25–28] or a persistent highly branched perfluoroalkyl radical[29]. These initiators require heating conditions (68 and 95 °C, respectively), leading to poly(FO-*alt*-VE) alternating copolymers with noteworthy thermal properties. This study aims at focusing on the use of TBB-MOPA/CH_3COOH system affording the desired poly(FO-*alt*-VE) copolymer in O_2-tolerant and room temperature (Scheme 1).

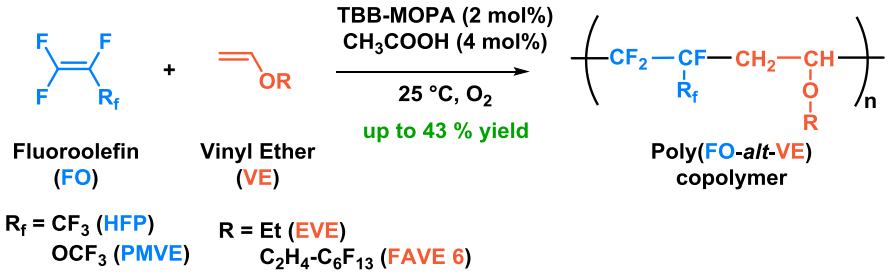

Scheme 1: Radical copolymerization of perfluoroolefins (FO) with vinyl ethers (VE) in presence of tri-nbutylborane methyloxypropylamine (TBB-MOPA).

2. Materials and Methods

Chemicals . Perfluoromethylvinyl ether (PMVE) was purchased at SynQuest, Florida, USA. Hexafluoropropene (HFP) was kindly offered by Arkema (Pierre-Bénite, France); 2-(perfluorohexyl)ethyl vinyl ether (FAVE6) by Unimatec Co., Ltd, Ibaraki, Japan; while tri-*n*butylborane methyloxypropylamine (TBB-MOPA) by CALLERY™ and 1,1,1,3,3-pentafluorobutane $C_4H_5F_5$ by Solvay, Tavaux, France. Ethyl vinyl ether (EVE), hexafluoroxylene, acetic acid, acetonitrile and diethyl ether were purchased from Aldrich Sigma, Apollo Scientific and VWR, and used without any further purification.

Nuclear magnetic resonance (NMR) spectroscopy. The ^{13}C, ^{1}H and ^{19}F NMR spectra were recorded on Bruker Avance 400 instruments, using $CDCl_3$ as deuterated solvent, the signal of which was locked at 7.26 ppm. DMSO-d_6 probe was also used when the copolymers were not soluble in usual deuterated solvents. Hexafluorobenzene was used as internal standard for ^{19}F and ^{1}H NMR analyses,

its signal being calibrated at -164.9 ppm. Coupling constants and chemical shifts are given in Hertz (Hz) and parts per million (ppm), respectively. The experimental conditions for recording ^{1}H [or ^{19}F] NMR spectra were as follows: angle 90° [or 30°], acquisition time 4.5 s [or 0.7 s], pulse delay 2 s [or 5 s], number of scans 36 [or 64], and a pulse width of 5 µs for ^{19}F NMR. ^{1}H NMR decoupling was applied on all ^{13}C NMR spectra and on Attached Proton Test mode ($^{13}C\{^{1}H\}$-APT).

For 2D NMR spectroscopy, HeteroCOSY ^{1}H-^{19}F spectra were obtained with 2048 points in the F1 (^{1}H) dimension and 5350 points in F2 (^{19}F) one, a spectral width of 5.2 kHz in F1 and 5.3 kHz in F2. Acquisition times were 0.20 s in F1 and 0.05 s in F2. Thirty two scans and a relaxation delay of 1 s were applied.

Thermogravimetric analysis (TGA). The thermogravimetric analysis of the copolymers (*ca.* 10 mg) was carried out under air with a TA Instruments TGA 51 apparatus. The polymer samples were heated from 20 to 550 °C at a heating rate of 10 °C min^{-1}. The apparent degradation temperature was defined at the point where the relative weight loss was about 5% and consequently named $T_{d5\%}$.

Fourier transform infrared (FTIR) spectroscopy. FTIR analyses of the copolymers were performed using a PerkinElmer Spectrum 1000 in ATR mode, with an accuracy of ±2 cm^{-1} and by the accumulation of 32 scans.

Size exclusion chromatography (SEC) measurements. Number average molar masses ($M_{n,sec}$) and dispersities (Đ) of the polymers were determined using a triple-detection GPC from Agilent Technologies with its corresponding Agilent software, dedicated to multi-detector GPC calculation. THF was used as the eluent at a flow rate of 0.8 mL min^{-1}, while polystyrene standards were used for the calibration. The system used two PL1113-6300 ResiPore 300 x 7.5 mm columns. The detector suite was composed of a PL0390-0605390 LC light scattering detector with two scattering angles (15° and 90°), a PL0390-06034 capillary viscometer, and a 390-LCPL0390-0601 refractive index detector. The entire SEC-HPLC system was thermostated at 35 °C. The typical sample concentration was 1 mg mL^{-1}.

Differential scanning calorimetry (DSC). DSC analyses of the different copolymers (*ca.* 10 mg) were carried out under N_2 atmosphere using a TA instruments Q100 instrument controlled with DSC 200 F3 software. The instrument was calibrated with noble metals and checked before analysis (indium sample for which T_m = 156.6 °C). After its insertion into the DSC apparatus, the polymer sample was cooled down from 20 °C to -100 °C and stabilized at the latter temperature for 10 min. Then, the first scan was performed at a heating rate of 10 °C min^{-1} from −100 °C up to 100 °C. This thermal cycle was repeated two more times. The glass transition temperature, T_g, was evaluated from the average value of the temperature taken at the half-height of the heat capacity drop using the method of

tangents for each run.

Dynamic mechanical analyses (DMA). DMA analyses were carried out on a Metravib Dynamic Mechanical Analyser (DMA 25®) driven with Dynatest 6.8 software. Solid samples were tested in uniaxial tension mode at a frequency of 1 Hz. First experiment consisted in determining the linear viscoelastic domain of each sample, i.e. the strain range for which the dynamic mechanical properties are independent of the strain imposed to the material. In such a way, a strain value of 0.01%, taken down in the linear domain, was retained for the conduction of consecutive thermomechanical test. In this analysis, the complex Young modulus E* = E' + j E" was measured as a function of temperature from *ca.* T_g - 100 °C up to T_g + 50 °C, at a heating rate of 3 °C min^{-1}. The real component E' is usually named "storage modulus" and is specific of the elastic contribution of the sample. In other words, it is proportional to the mechanical rigidity of the polymer. The imaginary part E" is named "loss modulus". It relates to the material ability for dissipating the mechanical energy.

Water contact angle (WCA). WCA measurements were carried out on Contact Angle System OCA-Data Physics. The water sessile drop method was used for the static contact angle (CA) measurements at ambient temperature. The probe liquid was water (θ_{H2O}) and the CA value was determined from average of five different drops of *ca.* 4.0 µL deposited on the same sample. Poly(PMVE-*alt*-EVE) and poly(HFP-*alt*-EVE) copolymers were prepared by pressing (Figures S5 and S6). Due to their softness, poly(PMVE-*alt*-FAVE6) and poly(HFP-*alt*- FAVE6) copolymers films were i) frozen in liquid nitrogen; ii) broken into pieces which were placed on glass; iii) warmed up to room temperature; iv) pressed by another glass to form a film; v) frozen in liquid nitrogen again to remove the second glass easily and vi) finally warmed up to room temperature.

Procedure:

Poly(PMVE-*alt*-EVE) copolymer. In a 50 mL autoclave, was introduced a mixture composed of ethyl vinyl ether (EVE, 8.00 g, 111 mmol, 48 mol%), TBB-MOPA (933 mg, 3.4 mmol, 1.5 mol%) and beforehand O_2-purged CH_3CN (30 mL). The autoclave was then closed and cooled down to -30 °C. The PMVE (20.00 g, 120 mmol, 52 mol%) was transferred into the autoclave (P = 1 bar) at that temperature. Under stirring, the mixture was warmed up to 0 °C (P = 2 bar) and the CH_3COOH (413 mg, 6.9 mmol, 2.9 mol%) diluted in CH_3CN (5 mL) was added into the mixture via a high pressure pump. After 16 h (T = 18 °C, P = 4 bar), the reaction was stopped. The copolymer, insoluble in CH_3CN (Figure S1a,b), was dissolved in Et_2O and precipitated from MeOH (Figure S1c). After drying at 60 °C under high-vacuum over 4 h, the poly(PMVE-*alt*-EVE) copolymer was obtained as a yellow and translucent waxy elastomer (10.95 g, 39 % yield) (Figure S1d).

Poly(PMVE-*alt*-FAVE6) copolymer. In the same conditions as above, a 50 mL autoclave containing FAVE6 (20.05 g, 51.8 mmol, 49 mol%), TBB-MOPA (542 mg, 2 mmol, 2 mol%) and O_2-purged CH_3CN (20 mL) was cooled down to -30 °C. Then, PMVE (9.2 g, 54.2 mmol, 51 mol%) was transferred in it (P = 1 bar). The mixture was stirred and warmed up to 0 °C (P = 2 bar) and CH_3COOH (240 mg, 4 mmol, 4 mol%) diluted in CH_3CN (5 mL) was injected. The reaction was stopped after 17 h (T = 24 °C, P = 2 bar). The copolymer (Figure S2a,b) was dissolved in 1,1,1,3,3-pentafluorobutane ($C_4H_5F_5$) and then precipitated from pentane (Figure S2c). After recovering the waxy product and drying at 60 °C under high-vacuum over 4 h, the poly(PMVE-*alt*-FAVE6) copolymer was obtained as a dark brown wax (12.36 g, 43 % yield) (Figure S2d).

Poly(HFP-*alt*-EVE) copolymer. In the same conditions as above, a 50 mL autoclave containing ethyl vinyl ether (EVE, 8.00 g, 111 mmol, 36 mol%), TBB-MOPA (1.2 g, 4.44 mmol, 1.4 mol%), O_2-purged CH_3CN (30 mL) was sealed and cooled to -30 °C. Then HFP (30 g, 200 mmol, 64 mol%) was transferred. After stirring and warming up to 0 °C (P = 3 bar), CH_3COOH (533 mg, 8.88 mmol, 2.8 mol%) diluted in CH_3CN (5 mL) was added into the mixture. After 3 h (T = 27 °C, P = 5 bar), the reaction was stopped. The copolymer (Figure S3a), insoluble in CH_3CN, was dissolved in Et_2O and precipitated from MeOH. After drying at 60 °C under high-vacuum over 4 h, the poly(HFP-*alt*-EVE) copolymer was obtained as a colorless amorphous material (3.35 g, 9 % yield) (Figure S3b).

Poly(HFP-*alt*-FAVE6) copolymer. In the same conditions as above, the autoclave containing FAVE6 (20.15 g, 51.8 mmol, 36 mol%), TBB-MOPA (542 g, 2 mmol, 1.4 mol%) and O_2-purged CH_3CN (20 mL). was cooled down to -30 °C. After transferring HFP (14 g, 93 mmol, 64 mol%), the mixture was warmed up to 0 °C (P = 1 bar) and CH_3COOH (240 mg, 4 mmol, 2.8 mol%) diluted in CH_3CN (5 mL) was added. After 6.5 h (T = 27 °C, P = 2 bar), the reaction was stopped. The copolymer (Figure S4a), partially soluble in CH_3CN, was dissolved in $C_4H_5F_5$ and precipitated from MeOH. After drying at 60 °C under vacuum over 4 h, the poly(HFP-*alt*-FAVE6) copolymer was obtained as a yellowish and translucent soft wax (5.63 g, 17 % yield) (Figure S4b).

3. Results and discussion

Though the literature reports many studies on the radical copolymerization of chlorotrifluoroethylene (CTFE)[22-29] or tetrafluoroethylene (TFE)[31] with VEs, to the best of our knowledge, only one patent claims the use of perfluoromethyl vinyl ether (PMVE)[35] and one article that of hexafluoropropylene (HFP).[27] In addition, terpolymerization of fluorinated olefins (FOs) with two different vinyl ethers (VEs) can be achieved either in presence of a radical initiator[25] or under visible-light irradiation.[30] In this work, mild polymerization conditions were studied using TBB-MOPA

as initiator with commercially available fluoroolefins (such as PMVE and HFP) and vinyl ethers [such as ethyl vinyl ether (EVE) and 2-(perfluorohexyl)ethyl vinyl ether (FAVE6)] monomers.

The experimental conditions of radical copolymerization of fluoroolefins with vinyl ethers, the molar masses, polydispersities as well as the degradation and glass transition temperatures of the obtained materials are summarized in Table 1.

Table 1 : Feed composition, molar mass and thermal properties of poly(FO-alt-VE) copolymers produced from radical copolymerizations[a] of fluorinated olefins (FOs) with vinyl ethers (VEs)

Entry	FO	VE	Feed compo-sition (FO (%) : VE (%))[a]	Copolymer compo-sition (FO (%) : VE (%)) [b]	Yield (%)	M_n (g mol^{-1})[c]	M_w	Đ ($\frac{M_w}{M_n}$) [c]	T_g (°C)	$T_{d5\%}$ (°C)
1	PMVE	EVE	52 : 48	45 : 55	39	70,000	169,200	2.42	-1	385
2	PMVE	FAVE6	51 : 49	50 : 50	43	nd[d]	nd[d]	nd[d]	-16	316
3	HFP	EVE	64 : 36	45 : 55	9	40,700	76,900	1.89	18	282
4	HFP	FAVE6	64 : 36	51 : 49	17	nd[d]	nd[d]	nd[d]	-15	262

[a] Polymerization conditions : TBB-MOPA (*ca.* 2 mol%), CH_3COOH (*ca.* 4 mol%), CH_3CN, 0 °C to 25 °C
[b] Copolymer composition was assessed from ^{19}F NMR spectroscopy
[c] Molar masses and polydispersities assessed from size exclusion chromatography (SEC) in THF calibrated with polystyrene standards.
[d] nd = not determined since the copolymer was not soluble in THF or warm DMF

Prior describing the resulting fluorinated copolymers, the low yields could be explained by the probable excess of oxygen. Actually, Chung et al. reported that the monooxidation of trialkylborane in catalytic oxygen content is essential in forming the active radicals for initiating the polymerization.[8–10] Though we have not quantified the O_2 content in the medium, it can be expected that the excess of oxygen not involved in that monooxidation might bring some inhibition of the copolymerization, hence making lower the yields. In addition, the difference in yields from the radical copolymerization of FO monomers arises from two features: i) the 1:1 stoichiometry in PMVE:VE feed (runs 1-2) led to the best copolymerization rate (in contrast to an excess of HFP in runs 3-4) and ii) the comparison of high e values of comonomers in absolute value (e_{EVE}= -1.80 *versus* that of PMVE to favor the alternance (e_{PMVE} = 3.01[31] >> e_{HFP}= 1.50[32]). A low yield was also reported for a copolymerization of HFP with another vinyl ether.[25]

NMR

Poly(PMVE-*alt*-EVE) copolymer. After reaction and purification, the copolymer was characterized by ^1H NMR spectroscopy, the spectrum of which (Figure 1a) shows: i) the absence of the signals around 6 ppm that evidences the good reactivity of EVE; ii) a singlet at 1.18 ppm, attributed to CH_3 in EVE unit; iii) large signals ranging from 2.37-2.99, 3.55-3.92 and 4.06-4.55 ppm, assigned to CH_2, O-CH_2

and CH,[25–28,36] respectively. The ^{19}F NMR spectrum (Figure 1b) exhibits a characteristic singlet at -52.20 ppm attributed to CF_3[37] and broad signals assigned to CF and CF_2 ranging from -130 to -110 ppm. The complexity of the latter is due to 2 chiral carbon centers -CF_2-C*F(OCF_3)-CH_2-CH*(OEt)-, making both protons in CH_2 and 2 F atoms in CF_2 non-equivalent. The PMVE : EVE ratio was determined with the use of hexafluoroxylene as internal standard, quantitatively relating the ^{1}H and ^{19}F NMR signal intensities of perfluorinated and non-fluorinated monomers units.

This allows to get PMVE : $C_6H_4(CF_3)_2$ and EVE : $C_6H_4(CF_3)_2$ ratios from the integrals of their characteristic signals in the ^{1}H and ^{19}F NMR spectra, respectively. By deduction, PMVE : EVE ratio was determined from Equation 1 as 45 : 55.

$$\frac{[PMVE]}{[EVE]} = \frac{[PMVE]}{[IS]} \times \frac{[IS]}{[EVE]} = \frac{\int_{-53.4}^{-51.2} CF_3(PMVE) \div 3}{\int_{-64.9}^{-61.5} (CF_3)_2\,(IS) \div 6} \times \frac{\int_{7.6}^{7.9} C_6H_4\,(IS) \div 4}{\int_{1.0}^{1.3} CH_3(EVE) \div 3} \qquad (1)$$

where [*IS*] and $\int_i^j CX_2$ stand for the internal standard concentration and the integral of the NMR signal assigned to CX_2 ranging from i to j ppm, respectively.

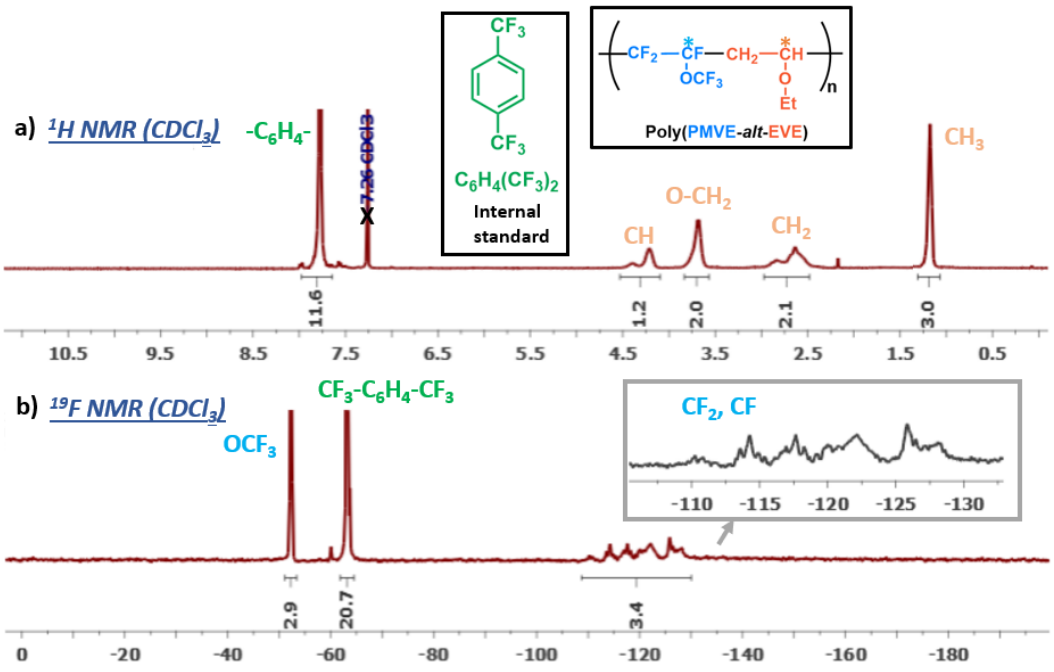

Figure 1 : ^{1}H (a) and ^{19}F (b) NMR spectra of poly(PMVE-alt-EVE) copolymer in $CDCl_3$ with hexafluoroxylene as the internal standard.

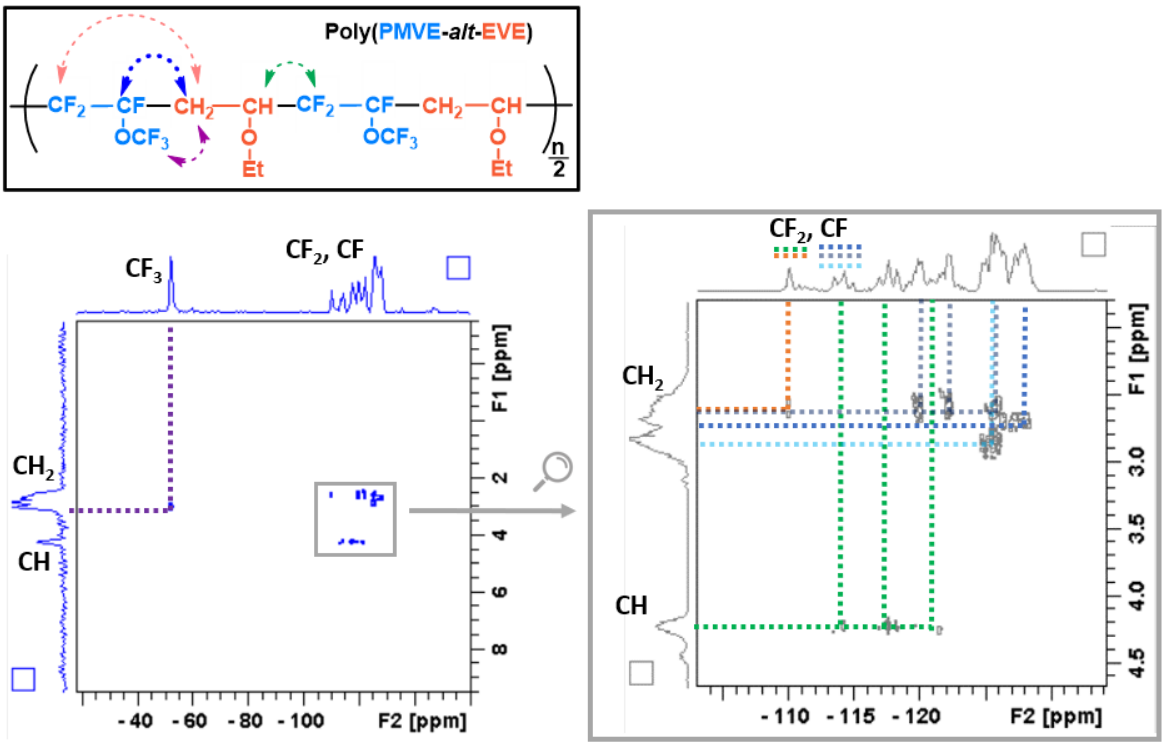

Figure 2 : HeteroCOSY ^{1}H-^{19}F NMR spectrum and its expansion (right) of poly(PMVE-alt-EVE) copolymer in $CDCl_3$. The one-dimensional spectra are plotted on the horizontal top (^{19}F) and vertical left (^{1}H) of the 2D plots.

The HeteroCOSY ^{1}H-^{19}F spectrum (Figure 2) displays a correlation (purple) between CH_2 (2.37-2.99 ppm) and CF_3 (-52.20 ppm), which should be a through-space coupling with the presence of oxygen atom in OCF_3 group. The CH_2 is also correlated to both CF (blue lines in different shades) and CF_2 (red line) signal groups, spread from -130 to -110 ppm. The aligned (green) signals correlation of CH (4.25 ppm) with CF_2 was also observed. It is worth noting that CH_2/CF (blue) correlations have a much stronger intensity than other ones. These assignments allow us to distinguish CF_2 and CF signals that was not possible from the ^{19}F NMR 1D spectra. Though to the best of our knowledge, such a HeteroCOSY spectrum of this copolymer has never been reported, deeper work is required to explain the tacticity in this structure.

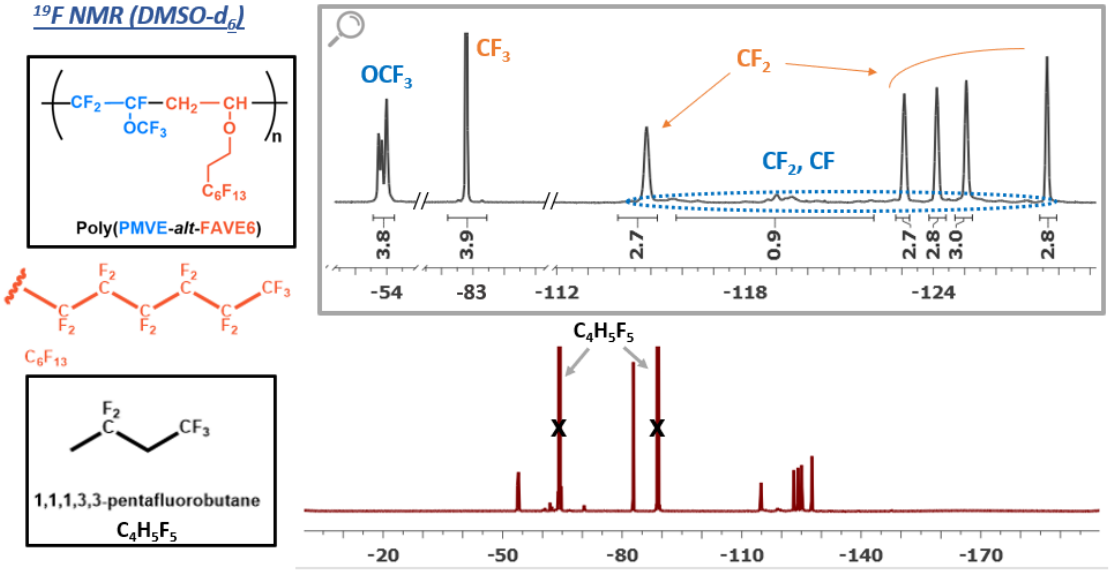

Figure 3 : ^{19}F NMR spectrum and its expansion in various ppm zones (top) of poly(PMVE-alt-FAVE6) copolymer in 1,1,1,3,3-pentafluorobutane with a DMSO-d_6 probe

Poly(PMVE-*alt*-FAVE6) copolymers. Poly(PMVE-*alt*-FAVE6) copolymer was dissolved in 1,1,1,3,3-pentafluorobutane ($C_4H_5F_5$) and characterized by NMR spectroscopy with a DMSO-d_6 probe. The ^1H NMR spectrum was not suitable for this analysis because of the presence of intense signals assigned to $C_4H_5F_5$ overlapping with those of FAVE6 units. The composition of that copolymer was then determined by ^{19}F NMR spectrum (Figure 3) that displays the characteristic signals of both monomer units. As above, the signals assigned to PMVE units are centered at -53.8 ppm (OCF_3) while the broad signal ranging from -105 to -130 ppm corresponds to its CF and CF_2 groups. As expected, the C_5F_{10} signals in FAVE6 units are located at -114.98, -123.1, -124.1, -125.1 and -127.6 ppm attributed to CF_2 moieties, while the CF_3 end-group displays a characteristic signal at -82.8 ppm. Based on the integrals of both CF_3 (in FAVE6) and OCF_3 (in PMVE) signals, the calculated PMVE : FAVE6 molar ratio was 1 : 1 and evidences the alternating structure of such a copolymer.

Poly(HFP-*alt*-EVE) copolymers. As for that of poly(PMVE-*alt*-EVE) copolymer, the ^1H NMR spectroscopy (Figure S13a) shows the absence of signals of the ethylenic protons in EVE monomer. It exhibits three signals at 4.23, 3.65 and 1.16 ppm, attributed to CH, $-OCH_2-$ and CH_3, respectively. The broad signal ranging from 3.11 to 2.22 ppm is assigned to CH_2 in the polymer backbone. The ^{19}F NMR spectra (Figure S13b) exhibits the characteristic signals of CF_3 and CF centered at -75.3 and -182.6 ppm, respectively, while the complex signal from -107.9 to -121.4 ppm is attributed to CF_2. Similarly to the case of poly(PMVE-*alt*-EVE) copolymer, the HFP : EVE ratio was determined from the use of hexafluoroxylene as internal standard in both NMR spectra (Equation 2), and is 45 : 55.

$$\frac{[HFP]}{[EVE]} = \frac{[HFP]}{[IS]} \times \frac{[IS]}{[EVE]} = \frac{\int_{-76.9}^{-74.9} CF_3(HFP) \div 3}{\int_{-63.6}^{-62.6} (CF_3)_2\ (IS) \div 6} \times \frac{\int_{7.6}^{7.9} C_6H_4(IS) \div 4}{\int_{1.0}^{1.3} CH_3(EVE) \div 3} \qquad (2)$$

Poly(HFP-*alt*-FAVE6) copolymers. As above, poly(HFP-*alt*-FAVE6) copolymer was dissolved in $C_4H_5F_5$ and characterized by NMR spectroscopy with a DMSO-d_6 probe. Though the absence of ethylenic protons of FAVE-6 monomer were absent, the ^{1}H NMR spectrum could not help in that characterization because of the intense signals of $C_4H_5F_5$. Similarly, the composition of that copolymer was assessed by the ^{19}F NMR spectrum (Figure 4) that shows the characteristic signals of both monomer units. As above, related to HFP units, the signal centered at -76 ppm is characteristic of CF_3 while the broad signals ranging from -110 to -121 ppm and from -182 to -186 pm were assigned to CF_2 and CF groups, respectively. The former broad signal comes from the non-equivalent fluorine atoms in alpha position about both asymmetric carbons in bulky ***C***F(CF_3) and ***C***H($OC_2H_4C_6F_{13}$) groups. Beside the signals of FAVE6 units located at -114.98, -123.1, -124.1, -125.1 and -127.6 ppm attributed to CF_2 moieties, that of the CF_3 group is low field shifted to -82.8 ppm. Based on the integrals of both CF_3 signals in both comonomers units, the calculated HFP : FAVE6 molar ratio was 1 : 1.

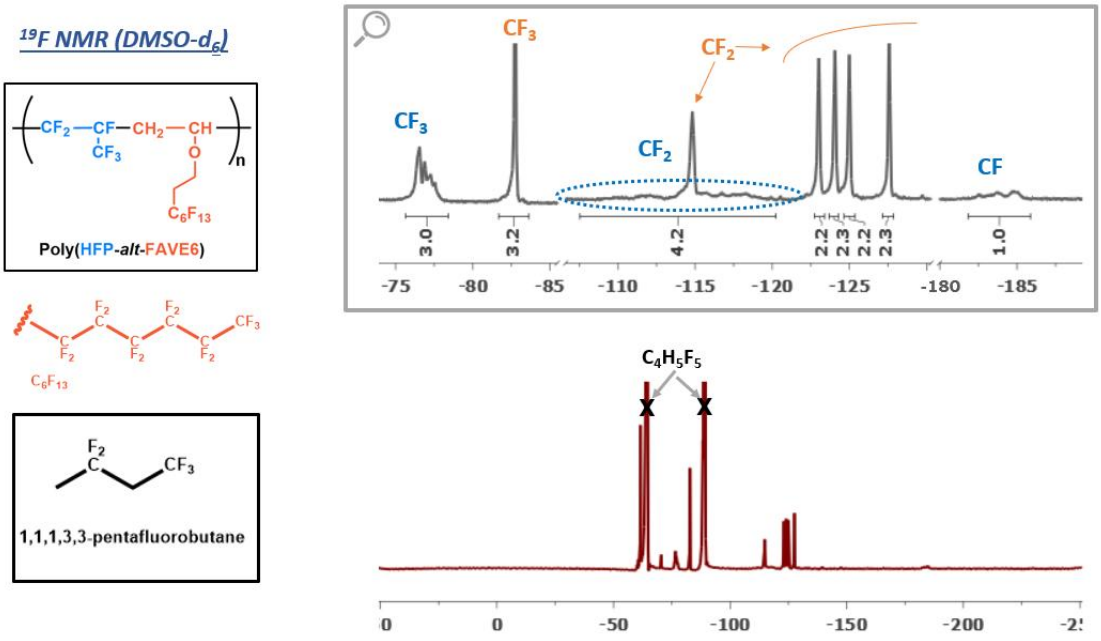

Figure 4: ^{19}F NMR spectrum and its expansion of poly(HFP-alt-FAVE6) copolymer in 1,1,1,3,3-pentafluorobutane with a DMSO-d_6 probe

Fourier transform infrared (FTIR) spectroscopy

Each FTIR spectrum of the four synthesized copolymers (Figure 5 and S12) displays three wide bands centered at *ca.* 2980, 2920 and 2850 cm^{-1}, corresponding to C(sp^3)-H bond. The C-H bands characteristic of poly(HFP-*alt*-EVE) copolymer present the highest amplitude, probably because of

the highest ratio of the number of C-H bonds upon the number of C-O and C-F bonds present in the polymer chemical backbone. The same explanation may be used to justify the particularly low intensity of the C-H band of poly(HFP-*alt*-FAVE6) copolymer.

Comparing the IR spectra of the four copolymers enabled the assignment of the C-F frequencies for PMVE, HFP and FAVE6. The overlapped C-F and C-O bands are found between 1300 and 1050 cm^{-1}. PMVE units exhibit C_F-O-C_F and C-F bands at 1093 cm^{-1} (green), 1230 and 1181 cm^{-1} (black). HFP units display C-F bands at 1228 and 1188 cm^{-1} (orange) while FAVE6 units exhibit C-F bands at 1140 cm^{-1} (blue), 1230 and 1181 cm^{-1} (black). Both EVE and FAVE6 have C_H-O-C_H bands at 1137 cm^{-1} (pink), present in all four FTIR spectra. It is worth noting that the C_H-O-C_H bands are as intense as C-F bands, though C-F bands are supposed to exhibit higher intensities because of the higher polarity and number of C-F bonds.

All these vibrations have stretching nature. The absence of C=C bands, that should be noted at ca. 1600 cm^{-1}, evidences the absence of the monomers.

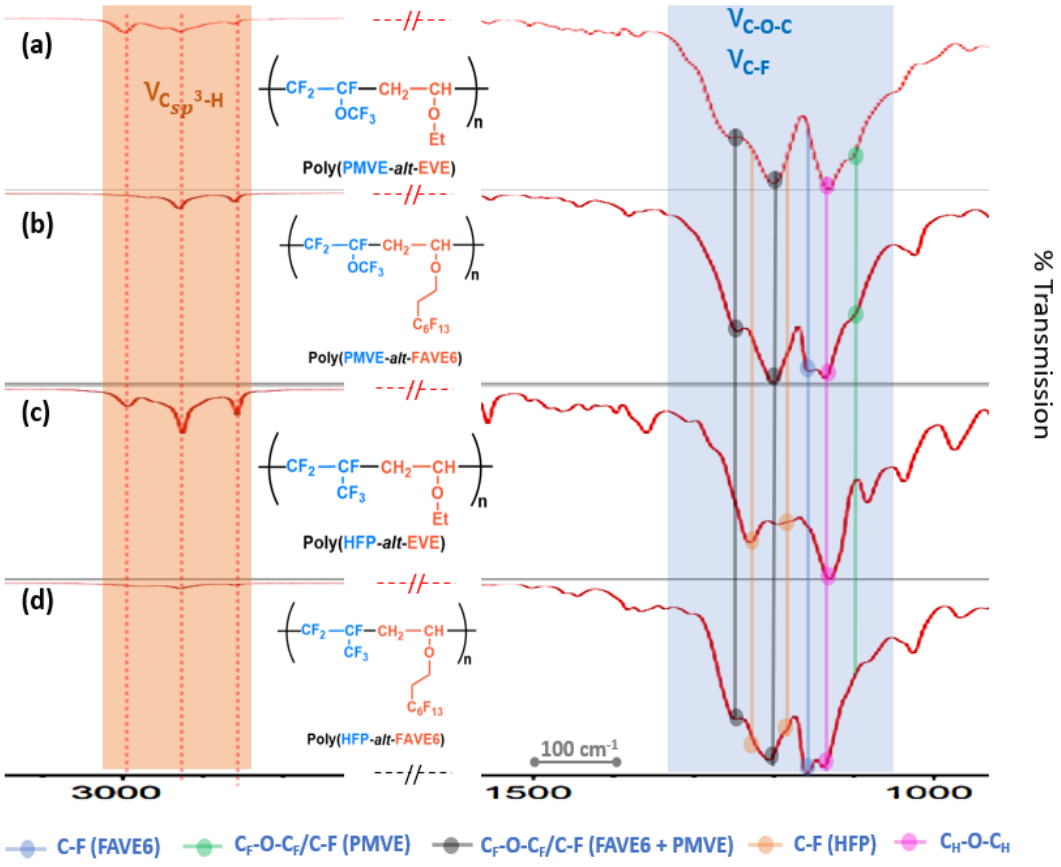

Figure 5: Expansion of FTIR spectra of (a) poly(PMVE-alt-EVE), (b) poly(PMVE-alt-FAVE6), (c) poly(HFP-alt-EVE) and (d) poly(HFP-alt-FAVE6) copolymers (the full spectra being supplied in the Supporting information).

Size Exclusion Chromatography (SEC)

As poly(PMVE-*alt*-FAVE6) and poly(HFP-*alt*-FAVE6) copolymers are not soluble in THF or DMF, only molar masses of poly(PMVE-*alt*-EVE) and poly(HFP-*alt*-EVE) copolymers could be determined by size exclusion chromatography (SEC) (Entries 1 and 3, Table 1, Figure S14) with reasonable molar masses (169,200 and 76,900 equivalent polystyrene, respectively, Table 1), especially when the comonomer feed was close to 1:1, as in the cases of the copolymers involving PMVE. As expected, for a conventional radical copolymerization, high dispersity values, Đ = 2.42 and 1.89, (even *quasi* bimodal for the former one, Figure S14), as well as molar mass, M_n = 70,000 and 40,700 g mol^{-1}, were observed for poly(PMVE-*alt*-EVE) and poly(HFP-*alt*-EVE) copolymers, respectively.

Thermogravimetry analysis (TGA)

The thermogravimetric analyses of the synthesized copolymers were performed under air (Figure 6). It is known that fluoroelastomers are a class of synthetic rubbers that exhibit resistance above 200 °C.[3,38,39] Such a behavior is observed here with our copolymers. Indeed, the thermal degradation of poly(PMVE-*alt*-FAVE6), poly(HFP-*alt*-EVE) and poly(HFP-*alt*-FAVE6) copolymers occurs at relatively high temperatures. The apparent degradation temperatures, $T_{d5\%}$, are close to 316, 282 and 262 °C, respectively. The highest thermostability is obtained with the poly(PMVE-*alt*-EVE) copolymer with an apparent degradation temperature close to $T_{d5\%}$ = 385 °C, probably due to its higher molar mass. This is not surprising since PFA (perfluoroalkoxy polymer), a copolymer based on tetrafluoroethylene (TFE) and PMVE, is more thermally stable than FEP [poly(TFE-co-HFP) copolymer].[40]

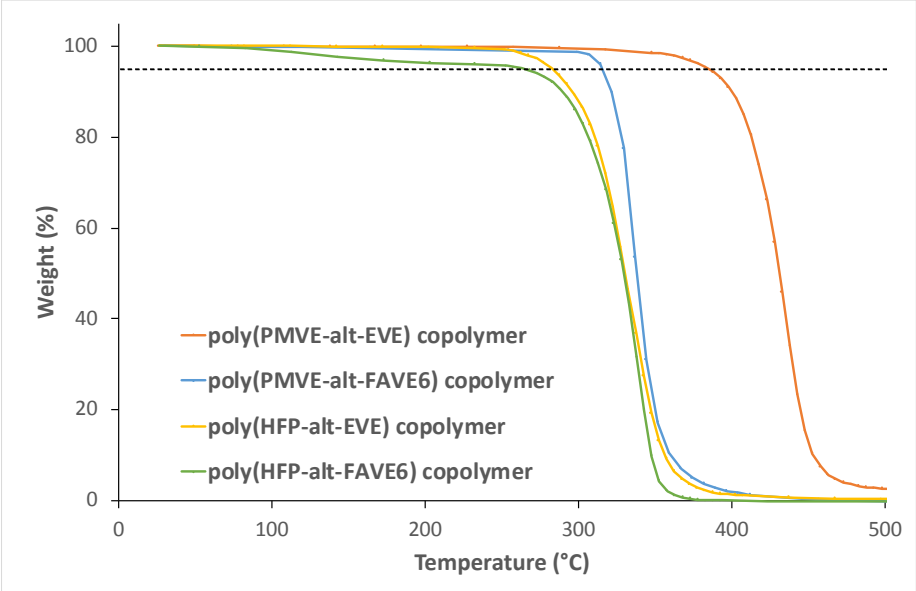

Figure 6 : TGA thermograms of poly(PMVE-alt-EVE) (red orange), poly(PMVE-alt-FAVE6) (blue), poly(HFP-alt-EVE) (yellow) and poly(HFP-alt-FAVE6) (green) copolymers under air. The dotted line shows the 5 wt% thermal decomposition of the copolymer.

Differential scanning calorimetry (DSC)

The calorimetric profiles of the four synthesized copolymers were evaluated by DSC in dynamic mode under inert atmosphere (N_2). The thermograms specific of poly(PMVE-*alt*-EVE) and poly(HFP-*alt*-EVE) copolymers are shown in Figures S7 and S9 while those characteristic of poly(PMVE-*alt*-FAVE6) and poly(HFP-*alt*-FAVE6) copolymers are represented in Figures S8 and S10, respectively. DSC thermograms of these copolymers revealed purely amorphous materials because no melting zone was observed. The glass transition temperature of each copolymer is reported in Table 1. The order of magnitude of these different T_g values is consistent with the data described in the literature with similar macromolecular systems.[36,41]

On an increasing T_g scale, the different materials can be classified as follows: poly(PMVE-*alt*-FAVE6) < poly(HFP-*alt*-FAVE6) < poly(PMVE-*alt*-EVE) < poly(HFP-*alt*-EVE). Such a hierarchy can be explained using structure-properties relationships. Indeed, the highest T_g value (18 °C) is observed with the most compact and most rigid chemical backbone based on HFP and EVE units . Keeping the EVE sequence, the replacement of HFP by PMVE induces a reduction of the T_g value to -1 °C (i.e. for poly(PMVE-*alt*-EVE) copolymer) due to the increase of the space between macromolecular chains. Indeed, the CF_3 side group present in HFP chemical structure is shorter than of the -O-CF_3 unit present in PMVE. Then, in this latter copolymer, the macromolecular cooperativity is lower and the presence of the oxygen atom brought some softness inducing a reduction of the T_g value compared to that of poly(HFP-*alt*-EVE). The same tendency is observed between poly(PMVE-*alt*-FAVE6) and poly(HFP-*alt*-FAVE6) copolymers. Steric considerations can also be used to explain the reduction in T_g that is detected when the EVE sequence is replaced by the much larger FAVE6 sequence. Then, the lowest T_g (-16 °C) is registered with the copolymer characterized by the most branched chemical backbone, i.e. the largest intermolecular space, for poly(PMVE-*alt*-FAVE6) copolymer. Nevertheless, the difference between both FAVE6-based copolymers is quite reduced because the length of the O-C_2H_4-C_6F_{13} side group hides the possible influence of the much shorter dangling unit present in HFP or PMVE sequence. Such a situation is summarized in Figure 7.

The influence of macromolecular size on the copolymer T_g value is identified as being much less important than the macromolecular free volume. Indeed, as discussed above (SEC section), the poly(PMVE-*alt*-EVE) copolymer is characterized by a M_n = 169,200 g mol^{-1} but its T_g is much reduced than that characteristic of poly(HFP-*alt*-EVE) copolymer with a M_n = 76,900 g mol^{-1}. In our study, the

distance between macromolecular chains is the most important parameter for influencing the copolymer T_g value.

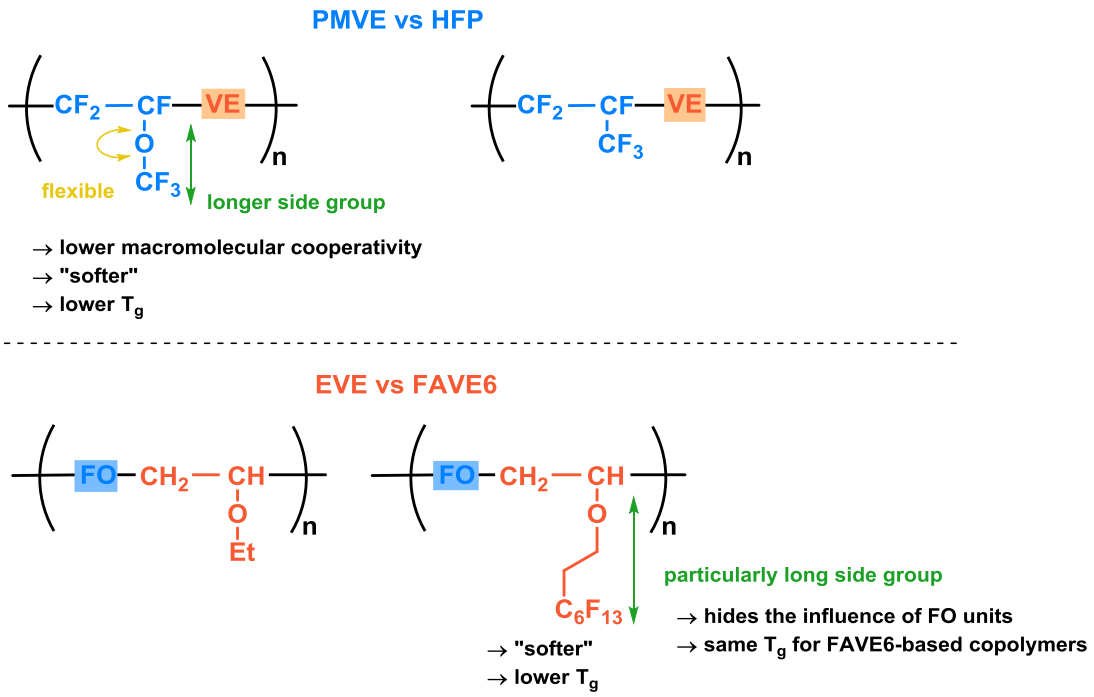

Figure 7: Comparison of structure-properties relationships between PMVE and HFP (top) and EVE and FAVE6 (bottom)

Dynamic Mechanical Analyses (DMA)

Poly(PMVE-*alt*-EVE) and poly(HFP-*alt*-EVE) copolymers exhibit a rubbery appearance at room temperature due to their low T_g. Their handling is quite easy for the production of rectangular samples as required for DMA tests (Figure S6)[35]. The other copolymers based on FAVE6 sequence present a pasty appearance at room temperature. This can be easily understood by the fact that they have an even lower T_g and especially are not crystalline.

After determination of the linear viscoelastic domain (Figure S11), the thermomechanical profile of poly(PMVE-*alt*-EVE) and poly(HFP-*alt*-EVE) copolymers was studied from -100 °C up to 50 °C. Figure 8a shows as example the data registered for the poly(PMVE-*alt*-EVE) copolymer. At low temperatures, the copolymer is in the glassy state with a high mechanical rigidity ($E' > 10^9$ Pa). The elastic character is predominant. Then, for T > 0 °C, the E' value sharply decreases in a limited temperature range. In the same area, the loss modulus E" describes a peak commonly called "α peak" that is characteristic of the main mechanical relaxation of macromolecular chains during the glass transition. Taken at its maximum, the T_α temperature is evaluated close to 7 °C. This temperature gives a rough evaluation of the copolymer T_g. Indeed, the T_α value depends on the frequency value used in the DMA test. But, in our case, the discrepancy between both temperatures

remains limited. Above the glassy transition, the sample is in a rubbery state. The storage modulus E' is still predominant, but its values are two decades lower than that in the glassy state.

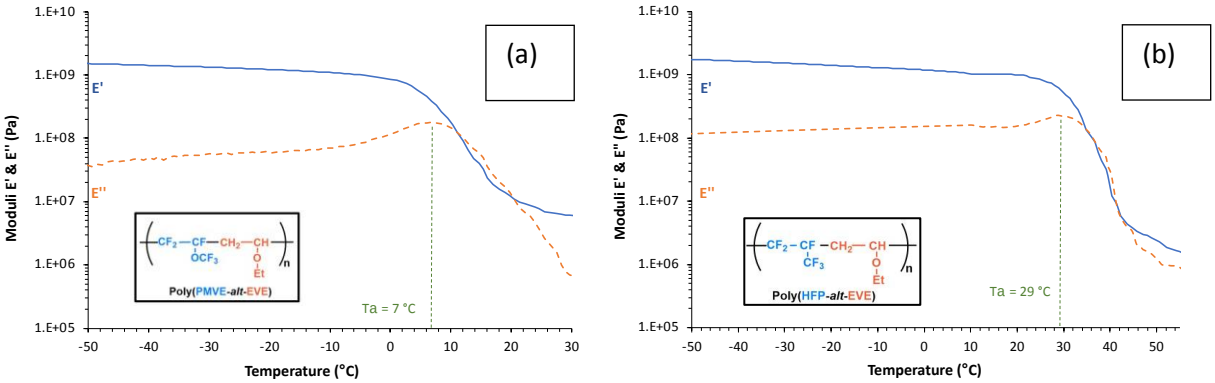

Figure 8 : DMA thermograms of poly(PMVE-alt-EVE) (graph a) and poly(HFP-alt-EVE) (graph b) copolymers with E' (blue curve) and E'' (orange curve) versus the temperature.

Similar phenomena can be observed in the thermomechanical profiles of poly(HFP-*alt*-EVE) copolymer (Figure 8b). The T_α temperature, taken at the maximum of the main mechanical relaxation peak is evaluated as being close to 29 °C. Once more, it is slightly higher than the T_g value (18 °C). It is noted that just above the glass transition temperature, Tg, the main relaxation peak observed in E" curve intersects the discontinuity registered in the E' curve. In other words, no crystalline plateau is detected but just a rubbery plateau. This characteristic is typical of a purely amorphous polymer. Indeed, in the case of a semi-crystalline polymer, the existence of the crystalline plateau, prevents the two curves of E' and E" from approaching each other in the glass transition region. Similar observation was noted with all copolymers studied here and that can be qualified as purely amorphous as evidenced by DSC experiments.

Water contact angle (WCA)

The surface properties of the synthesized copolymers were evaluated by means of water contact angle (WCA) measurements (Surprisingly, the contribution of FAVE6 is not so effective as it could have been anticipated, since the WCAs of poly(FO-*alt*-EVE) are slightly higher than those of poly(FO-*alt*-FAVE6) copolymers.

S1). A hydrophobic character was observed for the four copolymers with relatively similar measured WCAs, ranging from 95 to 110 °. This result is interesting because if the fluorinated chains are known to be hydrophobic, the presence of ether moieties likely disadvantage this characteristic properties.[42]

Beside the nature of the chemical groups present in each chemical skeleton, the influence of the average intermolecular distance is likely to being an influencing parameter as discussed previously

for explaining the hierarchy in T_g values. Indeed, the highest contact angle is observed with the poly(HFP-*alt*-EVE) copolymer that also presents the highest T_g value. The reverse situation is described with poly(PMVE-*alt*-FAVE6) copolymer characterized by the largest dangling molecular units and the lowest T_g value. In this latter case, the higher intermolecular distance (or higher free volume) makes it possible a slightly higher diffusion of water in the polymer matrix and consequently a "better" affinity with water. This peculiarity is likely at the origin of the lowest registered contact angle value. Surprisingly, the contribution of FAVE6 is not so effective as it could have been anticipated, since the WCAs of poly(FO-*alt*-EVE) are slightly higher than those of poly(FO-*alt*-FAVE6) copolymers.

Conclusion

This study reports the first oxygen-tolerant radical copolymerization of fluorinated and gaseous comonomers at room temperature, i.e. under non-conventional conditions, by using TBB-MOPA/CH_3COOH system. Different fluoroolefins and vinyl ethers, which do not homopolymerize under radical initiation, were successfully involved in this process, leading to various poly(FO-*alt*-VE) alternating copolymers in up to 43 % yield, clearly evidenced by IR and NMR spectroscopies. These fluorinated amorphous copolymers exhibit low T_g (-16 to 18 °C), hydrophobic surface (contact angle comprised between 95 and 110 °) and high thermostability ($T_{d5\%}$ up to 382 °C). The highest thermal stability is observed for poly(PMVE-*alt*-EVE) copolymer even if it does not present the highest T_g value that is observed for poly(HFP-*alt*-EVE) copolymer. The first characteristic is mainly governed by the polymer size while the second one is driven by the macromolecular stiffness. Our different data demonstrate the occurrence of an interesting copolymerization procedure in term of energy and easiness to handle, with simple oxygen introduction. Though the yields deserved to be increased by a better control of the oxygen content, all these points are of first importance for supporting a possible transfer to industrial scale. Further studies i) to improve the copolymerization yields, ii) to expand to other fluorinated monomers (e.g. CTFE and VDF) and iii) involving more complex procedures (*i.e*. controlled radical copolymerization as RAFT and iodine transfer polymerization) are under study. Such fluorinated copolymers are potential candidates in paints and coatings or elastomers.

Conflicts of interest

The authors declare that there is no conflict of interest.

Supporting Information

IR and NMR spectra; pictures of films used for DMA; DSC thermograms of poly(FO-*alt*-VE) copolymers; tables of WCA values; SEC chromatograms of poly(PMVE-*alt*-EVE); these items can be found in https://pubs.acs.org/journal/aapmcd.

Acknowledgments

The authors thank the Arkema (Pierre-Bénite, France), Unimatec (Ibaraki, Japan), CALLERY™ Borane (Bellevue, WA, USA) and Solvay (Tavaux, France) Companies for supplying free samples of hexafluoropropene (HFP), 2-(perfluorohexyl)ethyl vinyl ether (FAVE6), tri-*n*butylborane methyloxypropylamine (TBB-MOPA) and 1,1,1,3,3-pentafluorobutane, respectively.

References

(1) Holding, S. Technology of Fluoropolymers. *Chromatographia* **2010**, *71* (1–2), 173–173. https://doi.org/10.1365/s10337-009-1422-3.

(2) Smith, D. W.; Iacono, S. T.; Iyer, S. S. *Handbook of Fluoropolymer Science and Technology*; John Wiley & Sons, Inc.: Hoboken, NJ, USA, 2014. https://doi.org/10.1002/9781118850220.

(3) Drobny, J. G. Compounds for Automotive Fuel Systems. In *Fluoroelastomers Handbook*; Elsevier, 2016; pp 471–482. https://doi.org/10.1016/B978-0-323-39480-2.00013-0.

(4) Ameduri, B.; Sawada, H. *Fluorinated Polymers*; RSC, Cambridge, 2017.

(5) Ameduri, B.; Fomin, S. *Fascinating Fluoropolymers and Their Applications*; Elsevier, Oxford, 2020.

(6) Ameduri, B.; Fomin, S. *Opportunities for Fluoropolymers*; Elsevier, Oxford, 2020.

(7) Sianesi, D.; Caporiccio, G. Polymerization and Copolymerization Studies on Vinyl Fluoride. *J. Polym. Sci. Part A-1 Polym. Chem.* **1968**, *6* (2), 335–352. https://doi.org/10.1002/pol.1968.150060204.

(8) Zhang, Z.-C.; Chung, T. C. M. Reaction Mechanism of Borane/Oxygen Radical Initiators during the Polymerization of Fluoromonomers. *Macromolecules* **2006**, *39* (16), 5187–5189. https://doi.org/10.1021/ma061393a.

(9) Zhang, Z.-C.; Wang, Z.; Chung, T. C. M. Synthesis of Chain End Functionalized Fluoropolymers by Functional Borane Initiators and Application in the Exfoliated Fluoropolymer/Clay Nanocomposites. *Macromolecules* **2007**, *40* (15), 5235–5240. https://doi.org/10.1021/ma070588v.

(10) Zhang, Z.-C.; Chung, T. C. M. Borane-Mediated Radical Polymerization; Preparation of Fluoropolymers for High Energy Density Capacitors; 2009; pp 331–344. https://doi.org/10.1021/bk-2009-1024.ch022.

(11) Lin, W.; Niu, H.; Chung, T. C. M.; Dong, J.-Y. Borane Chain Transfer Reaction in Olefin

Polymerization Using Trialkylboranes as Chain Transfer Agents. *J. Polym. Sci. Part A Polym. Chem.* **2010**, *48* (16), 3534–3541. https://doi.org/10.1002/pola.24125.

(12) Roberts, B. P. Polarity-Reversal Catalysis of Hydrogen-Atom Abstraction Reactions: Concepts and Applications in Organic Chemistry. *Chem. Soc. Rev.* **1999**, *28* (1), 25–35. https://doi.org/10.1039/a804291h.

(13) Rablen, P. R.; Hartwig, J. F. Accurate Borane Sequential Bond Dissociation Energies by High-Level Ab Initio Computational Methods. *J. Am. Chem. Soc.* **1996**, *118* (19), 4648–4653. https://doi.org/10.1021/ja9542451.

(14) Mottus, E. H.; Fields, J. E. Process for Polymerizing Unsaturated Monomers with a Catalyst Comprising an Organoboron Compound, a Peroxygen Compound and an Amine. US3275611A, 1966.

(15) Wilson, O. R.; Magenau, A. J. D. Oxygen Tolerant and Room Temperature RAFT through Alkylborane Initiation. *ACS Macro Lett.* **2018**, *7* (3), 370–375. https://doi.org/10.1021/acsmacrolett.8b00076.

(16) Timmins, R. L.; Wilson, O. R.; Magenau, A. J. D. Arm-first Star-polymer Synthesis in One-pot via Alkylborane-initiated RAFT. *J. Polym. Sci.* **2020**, *58* (10), 1463–1471. https://doi.org/10.1002/pol.20200089.

(17) Wilson, O. R.; McDaniel, R. M.; Rivera, A. D.; Magenau, A. J. D. Alkylborane-Initiated Thiol-Ene Networks for the Synthesis of Thick and Highly Loaded Nanocomposites. *ACS Appl. Mater. Interfaces* **2020**, *12* (49), 55262–55268. https://doi.org/10.1021/acsami.0c16587.

(18) Sonnenschein, M.; Webb, S.; Rondan, N. Amine Organoborane Complex Polymerization Initiators and Polymerizable Compositions. US2002025381A1, 2002.

(19) Jäkle, F. *New Polymeric Materials Based on Element-Blocks*; Chujo, Y., Ed.; Springers, Singapore, 2019. Chapter 4: Borylated Polystyrenes as Versatile Functional Materials, pp 59-76.

(20) Lalevée, J.; Povie, G.; Tehfe, M. A.; Telitel, S.; Morlet-Savary, F.; Graff, B.; Fouassier, J. P. Phototriggered In-Situ Generation of Triethylborane for Polymer Synthesis Under Air. *Macromol. Chem. Phys.* **2012**, *213* (15), 1618–1622. https://doi.org/10.1002/macp.201200186.

(21) Kojima, G.; Yamabe, M. Fluororesin for Solvent-Soluble Paint. *J. Synth. Org. Chem. Japan* **1984**, *42* (9), 841–849. https://doi.org/10.5059/yukigoseikyokaishi.42.841.

(22) Boutevin, B.; Cersosimo, F.; Youssef, B. Studies of the Alternating Copolymerization of Vinyl Ethers with Chlorotrifluoroethylene. *Macromolecules* **1992**, *25* (11), 2842–2846. https://doi.org/10.1021/ma00037a009.

(23) Takakura, T. *Modern Fluoropolymers*; Scheirs, J., Ed.; Wiley, New York, 1997. Chapter 29 : CTFE/Vinyl Ether Copolymers, pp 557– 564.

(24) Gaboyard, M.; Hervaud, Y.; Boutevin, B. Photoinitiated Alternating Copolymerization of Vinyl Ethers with Chlorotrifluoroethylene. *Polym. Int.* **2002**, *51* (7), 577–584. https://doi.org/10.1002/pi.902.

(25) Valade, D.; Boschet, F.; Améduri, B. Synthesis and Modification of Alternating Copolymers Based on Vinyl Ethers, Chlorotrifluoroethylene, and Hexafluoropropylene. *Macromolecules* **2009**, *42* (20), 7689–7700. https://doi.org/10.1021/ma900860u.

(26) Tayouo, R.; David, G.; Améduri, B.; Rozière, J.; Roualdès, S. New Fluorinated Polymers Bearing

Pendant Phosphonic Acid Groups. Proton Conducting Membranes for Fuel Cell. *Macromolecules* **2010**, *43* (12), 5269–5276. https://doi.org/10.1021/ma100703k.

(27) Alaaeddine, A.; Boschet, F.; Ameduri, B.; Boutevin, B. Synthesis and Characterization of Original Alternated Fluorinated Copolymers Bearing Glycidyl Carbonate Side Groups. *J. Polym. Sci. Part A Polym. Chem.* **2012**, *50* (16), 3303–3312. https://doi.org/10.1002/pola.26112.

(28) Alaaeddine, A.; Couture, G.; Ameduri, B. An Efficient Method to Synthesize Vinyl Ethers (VEs) That Bear Various Halogenated or Functional Groups and Their Radical Copolymerization with Chlorotrifluoroethylene (CTFE) to Yield Functional Poly(VE-Alt-CTFE) Alternated Copolymers. *Polym. Chem.* **2013**, *4* (16), 4335. https://doi.org/10.1039/c3py00443k.

(29) Puts, G.; Lopez, G.; Ono, T.; Crouse, P.; Ameduri, B. Radical Copolymerisation of Chlorotrifluoroethylene with Isobutyl Vinyl Ether Initiated by the Persistent Perfluoro-3-Ethyl-2,4-Dimethyl-3-Pentyl Radical. *RSC Adv.* **2015**, *5* (52), 41544–41554. https://doi.org/10.1039/C5RA05066A.

(30) Quan, Q.; Ma, M.; Wang, Z.; Gu, Y.; Chen, M. Visible-Light-Enabled Organocatalyzed Controlled Alternating Terpolymerization of Perfluorinated Vinyl Ethers. *Angew. Chemie Int. Ed.* **2021**, anie.202107066. https://doi.org/10.1002/anie.202107066.

(31) Ameduri, B.; Boutevin, B. *Well-Architectured Fluoropolymers: Synthesis, Properties And Applications*; 2004. Table 1, page 190.

(32) Moggi, G.; Bonardelli, P.; Russo, S. Emulsion Polymerization of the Vinylidene Fluoride-Hexafluoropropene System. *Conv. Ital. Sci. Macromol.* **1983**, *2*, 405–408.

(33) Hoshino, T.; Morizawa, Y. Chapter 5. Fluorinated Specialty Chemicals - Fluorinated Copolymers for Paints and Perfluoropolyethers for Coatings. In *Fluorinated Polymers*; Ameduri, B., Sawada, H., Eds.; 2017; pp 110–126. https://doi.org/10.1039/9781782629368-00110.

(34) Tabata, Y.; Du Plessis, T. A. Radiation-Induced Copolymerization of Chlorotrifluoroethylene with Ethyl Vinyl Ether. *J. Polym. Sci. Part A-1 Polym. Chem.* **1971**, *9* (12), 3425–3435. https://doi.org/10.1002/pol.1971.150091202.

(35) Shimada, M.; Sakagami, T.; Shiho, H.; Hashiguchi, Y. A Coating Composition, and a Coated Film and Glass Each Having a Coating Layer Comprised Thereof. EP1054047A2, 2000.

(36) Carnevale, D.; Wormald, P.; Ameduri, B.; Tayouo, R.; Ashbrook, S. E. Multinuclear Magnetic Resonance and DFT Studies of the Poly(Chlorotrifluoroethylene- Alt -Ethyl Vinyl Ether) Copolymers. *Macromolecules* **2009**, *42* (15), 5652–5659. https://doi.org/10.1021/ma900789t.

(37) Boyer, C.; Ameduri, B.; Hung, M. H. Telechelic Diiodopoly(VDF- Co -PMVE) Copolymers by Iodine Transfer Copolymerization of Vinylidene Fluoride (VDF) with Perfluoromethyl Vinyl Ether (PMVE). *Macromolecules* **2010**, *43* (8), 3652–3663. https://doi.org/10.1021/ma100207h.

(38) Drobny, J. G.; Moore, A. L. *Fluoroelastomers Handbook*; William Andrew, N. Y., Ed.; 2005.

(39) Drobny, J. G. *Fluoroelastomers Handbook, The Definitive User's Guide*, 2nd ed.; William Andrew Publishing, Oxford, 2016.

(40) Drobny, J. *Specialty Thermoplastics*; Drobny, J., Ed.; Springer, Berlin, Heidelberg, 2015; Vol. 13. https://doi.org/10.1007/978-3-662-46419-9.

(41) Friedman, M.; Walsh, G. High Performance Films: Review of New Materials and Trends. *Polym. Eng. Sci.* **2002**, *42* (8), 1756–1788. https://doi.org/10.1002/pen.11069.

(42) Delucchi, M.; Turri, S.; Barbucci, A.; Bassi, M.; Novelli, S.; Cerisola, G. Fluoropolyether Coatings: Relationships of Electrochemical Impedance Spectroscopy Measurements, Barrier Properties, and Polymer Structure. *J. Polym. Sci. Part B Polym. Phys.* **2002**, *40* (1), 52–64. https://doi.org/10.1002/polb.10069.

Table of Contents